Fluorimetric Nerve Gas Sensing Based on Pyrene Imines Incorporated into Films and Sub-Micrometer Fibers

By *Jeremy M. Rathfon, Zoha M. AL-Badri, Raja Shunmugam, Scott M. Berry, Santosh Pabba, Robert S. Keynton, Robert W. Cohn,* and *Gregory N. Tew**

The chemical sensing of nerve gas agents has become an increasingly important goal due to the 1995 terrorist attack in a Tokyo subway as well as national security concerns in regard to world affairs. Chemical detection needs to be sensitive and selective while being facile, portable, and timely. In this paper, a sensing approach using a pyrene imine molecule is presented that is fluorimetric in response. The detection of a chloro-Sarin surrogate is measured at 5 ppmv in less than 1 second and is highly selective towards halogenated organophosphates. The pyrene imine molecule is incorporated into polystyrene films as well as micrometer and sub-micrometer fibers. Using both a direct drawing approach and electrospinning, micrometer and nanofibers can be easily manufactured. Applications for functional sensing micrometer and nanofibers are envisioned for optical devices and photonics in addition to solution and airflow sensing devices.

1. Introduction

Organophosphates are toxic compounds found in chemical-warfare agents, such as Sarin and Soman, as well as pesticides. Highly active, volatile chemical-warfare nerve agents cause rapid and severe inhibition of serine proteases, most markedly acetylcholinesterase, which is vital to nerve function. This inhibition is often fatal. Nerve agents were used in the 1995 terrorist attack in a Tokyo Subway[1] and on Kurdish communities in Iraq.[2] The ease of manufacturing and dispensability, as well as available, inexpensive starting materials make these agents a weapon of choice for criminal terrorist attacks. Thus, the rapid sensing of these nerve agents has become an increasingly important research goal, especially aimed towards practical ''in the field'' devices. Concerns for national security as well as large stockpiles of aging and currently leaking weapons containing nerve agents in the United States make the problem of nerve agent sensing even more imperative.[3]

There have been a number of approaches for the detection of chemical-warfare agents including colorimetric,[4–6] fluorimetric,[7–12] photoacoustic spectroscopy,[13] gas chromatography-mass spectrometry,[14] enzymatic assays,[15] and molecular imprinting coupled with lanthanide luminescence and fiber optics.[16] Although all of these methods have advantages and disadvantages, no gold standard has emerged and many approaches are either complex, non-sensitive, non-selective, or do not sense in real time. Continued improvements in the detection of warfare agents are critical. Key attributes of a practical sensing system are sensitivity, selectivity, timely detection, and portability along with operational simplicity. An extremely facile method of chemical sensing is the creation of an optical event, such as a color change or fluorescence, upon exposure to an analyte, referred to as ''turn on'' sensors.[5–7,9,12,17,18] The very high sensitivities of fluorescence based sensing molecules make this mode of detection particularly attractive.[7,18]

This report shows the fluorimetric detection of nerve agent surrogates in both solution and functional micrometer and sub-micrometer fibers (Fig. 1). The pyrene imine molecules (Fig. 2) used for sensing are weakly luminescent in the UV region, but upon exposure to a nerve agent mimic the molecules fluoresce strongly in the visible spectrum. The sensing scheme is simple and robust, being able to detect nerve agent mimics in the vapor phase from a solid support. The sensitivity and selectivity of the pyrene imine and how these properties change in the solution and bulk polymer films as well as fibers are discussed.

Recent studies have shown the use of nanofibers and other nanoobjects as useful architectures for many applications such as tissue engineering, photonics, catalysis, electronics, optics, scaffolds for microfluidics,[19–21] and, most pertinently, sensing.[22–25] There are a few accessible techniques to manufacture polymer nanofibers including electrospinning.[26] Recently, Cohn and associates produced multiple oriented, suspended polymer nanofibers in parallel via a facile direct drawing approach.[20,27] The creation of fibers increases detection surface area and thus

[*] Prof. G. N. Tew, J. M. Rathfon, Dr. Z. M. AL-Badri, R. Shunmugam
Department of Polymer Science and Engineering
University of Massachusetts Amherst
120 Governors Drive, Amherst, MA 01003 (USA)
E-mail: tew@mail.pse.umass.edu
S. M. Berry, S. Pabba, Prof. R. S. Keynton, Prof. R. W. Cohn
ElectroOptics Research Institute and Nanotechnology Center
University of Louisville
Louisville, KY 40292 (USA)

DOI: 10.1002/adfm.200800947

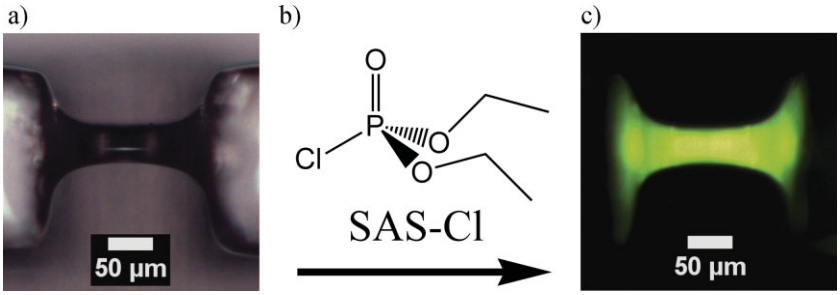

Figure 1. Detection scheme of a nerve agent mimic with the pyrene imine **1**. Fibers were formed from 15 wt % PS in toluene, containing 0.1 wt % **1**, before (left) and after (right) exposure to SAS-Cl.

could lead to an increase in response time and sensitivity.[25,28] In addition to increased sensitivity, fibers can also be incorporated into devices for sensing applications. This report will discuss the sensitivity and selectivity of polymer fibers created both by electrospinning and the direct drawing approach.

Because of the health hazards involved with nerve agents, surrogates are commonly used and were chosen for the detection experiments reported here; diethyl chlorophosphate, chloro-Sarin surrogate (SAS-Cl), was chosen as a structural and functional mimic for the nerve agent Sarin, likewise pinacolyl methylphosphonate, Soman surrogate (SOS), was used as a mimic for Soman (Fig. 3).[6,7,10–12] Also shown in Figure 3 are various organophosphates and acetyl chloride (AcCl) which were chosen to test the selectivity of **1** for nerve agents versus compounds with similar structure and functionality.

2. Results and Discussion

The norbornene pyrene imine monomer (**1**) was synthesized in the pursuit of creating polymeric based sensors.[11,29] Monomer **1** was subjected to ring-opening metathesis polymerization (ROMP) yielding a homopolymer of densely packed pyrene functionalities, with the idea of using these polymers to directly draw fibers. However, these polymers exhibited the well-known excimer emission common to pyrene, so they only served as ''turn-off'' indicators in the presence of SAS-Cl. The ''turn off'' event is a decrease in intensity of emission and is more difficult to measure or see optically than the creation of a unique optical event. Further complicating the matter, the homopolymer of **1** has issues with solubility in many solvents. In order to create drawn fibers from polymers of molecular weight around 100 kDa, solutions at a minimum of 15 wt % need to be used to prevent fiber breakup.[30] The homopolymer is only minimally soluble (less than 1 wt %) in suitable, high vapor pressure drawing solvents such as toluene, chlorobenzene, and $CHCl_3$. To circumvent these difficulties we considered the direct use of monomer **1** itself. This structure proved to be a valuable ''turn on'' sensor as presented below.

2.1. Solution Properties of 1 and 2

Due to these complications with the homopolymer, the solution and bulk properties of the small molecule **1** were studied. This monomer was found to have much better sensing properties and capabilities with the creation of a unique ''turn on'' optical event, rather than the difficulties involved with a ''turn off'' sensing probe where a small decrease in a large signal must be detected. In addition, **1** can also be easily incorporated into polymer solutions for the purpose of drawing micrometer and submicrometer fibers. Studying the solution and bulk properties of **1** gave more insight on its sensing properties, and allows for the incorporation of **1** into future polymer compositions and architectures. To be sure the pyrene imine was essential for fluorimetric detection of nerve agents a model compound (**2**),

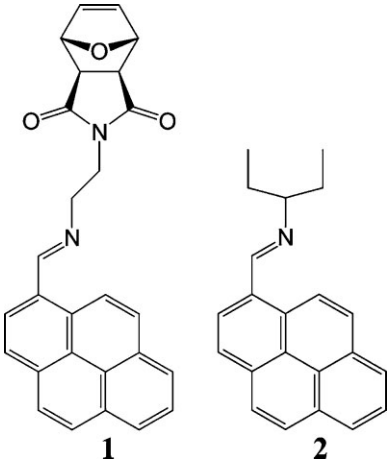

Figure 2. Chemical structures of the sensing molecules **1**, which is able to be polymerized, and **2**, a model compound.

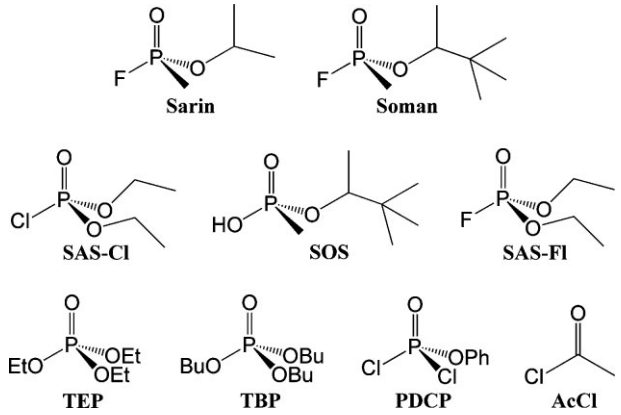

Figure 3. Chemical structures of the nerve agents Sarin (GB) and Soman (GD), the nerve agent mimics diethyl fluorophosphates (fluoro-Sarin surrogate (SAS-F)), diethyl chlorophosphate (chloro-Sarin surrogate (SAS-Cl)), and pinacolyl methylphosphonate (Soman surrogate (SOS)), as well as triethyl phosphate (TEP), tributyl phosphate (TBP), phenyl dichlorophosphate (PDCP), and acetyl chloride (AcCl).

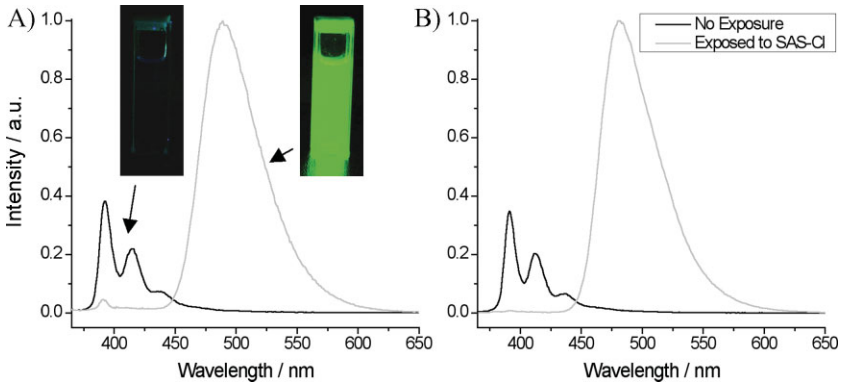

Figure 4. FL spectra of **1** (A) and **2** (B) in toluene before and after exposure to a large excess (20 μL) of SAS-Cl.

containing an alkyl group in place of the norbornene functionality, was also investigated.

The sensitivity and selectivity of both the norbornene pyrene imine (**1**) and the alkyl pyrene imine (**2**) were determined. Solutions were made of 1×10^{-4} wt % **1** and **2** in toluene. Fluorescence (FL) (Fig. 4) and UV-Vis (Fig. S1, Supporting Information) spectra were taken of both before and after exposure to a large excess (20 μL) of SAS-Cl. The FL and UV-Vis spectra of **1** and **2** are essentially identical. This equality in the spectra of **1** and **2** shows that the norbornene functionality has no effect on the optical properties of the pyrene imine group. Upon exposure to SAS-Cl, a red shift is seen in both the absorption and emission of the pyrene imine compounds. Most importantly, the emission of **1** shifts from a characteristic non-visible, UV pyrene emission to an intense visible green emission at approximately 490 nm instantaneously, allowing for the timely detection of SAS-Cl via a fluorimetric route.

NMR experiments were performed in order to further understand the interaction of SAS-Cl with the pyrene imine compounds. It is proposed that the interaction involves a primary nucleophilic attack of the imine nitrogen on the SAS-Cl phosphorous, followed by rearrangement to form a carbon-phosphorous bond at the imine group carbon. This proposed reaction is supported in other reports.[31] Monitoring this reaction with ^{1}H NMR, a decrease in the imine proton peak intensity (8.44 ppm) is seen which corresponds to the loss of this proton during the reaction. Expected shifts of the *β*-pyrene proton (8.89 ppm) as well as the proton adjacent to the imine (methylene in **1**, 4.01 ppm, and methyne proton in **2**, 3.12 ppm) confirm the phosphorylation of the imine. The corresponding ^{1}H NMR spectrum of the reacted pyrene imine is given in the Supporting Information (Fig. S14). The resultant phosphorylated imine bond is conjugated with the pyrene ring resulting in the observed red-shift in the fluorescence.

To further investigate the importance of the imine in the reaction with SAS-Cl, the UV-vis and FL spectra of 1-pyrenecarboxaldehyde, the aldehyde precursor to **1**, were also taken before and after exposure to SAS-Cl (Fig. S2). The spectra of the 1-pyrenecarboxaldehyde upon exposure to SAS-Cl, shows no observed decrease in the characteristic pyrene peaks and no green emission in the 490 nm range as observed with the reaction of SAS-Cl and **1**. This lack of detection on the part of 1-pyrenecarboxaldehyde shows that the reactive imine of **1** is crucial in the detection of SAS-Cl. The UV-Vis and FL spectra of **1**, before and after exposure to SAS-Cl, were also taken in DMSO and $CHCl_3$ and are similar to the toluene spectra in Figure 4.

The sensitivity of **1** in solution was determined by adding specific amounts of SAS-Cl and measuring the subsequent emission (Fig. 5). The green emission at approximately 490 nm can be detected both by the naked eye under a handheld UV lamp and through FL at an exposure of 40 parts per million volume (ppmv) SAS-Cl in both toluene and $CHCl_3$ (Fig. S3) at a concentration of 1×10^{-4} wt % of **1**. As more SAS-Cl is added, the characteristic pyrene peaks decrease and the green emission increases. The sensitivity of **2** (Fig. S4) was similar to that of **1**, however **2**, due to its lower molecular weight, had a slightly higher mole percent in solution, thus was slightly more sensitive at the same concentration (0.1 wt %).

2.2. Bulk PS Film Properties

In order to investigate the detection of nerve agents in the solid state and eventually in polymeric fibers, films were created of **1** dispersed in PS. The films and fibers were cast from a 15 wt % solution of PS in toluene containing 0.1 wt % **1**. The sensitivity and selectivity of these PS films were studied to determine their sensing properties. The green emission, and thus the sensitivity of **1**, in the PS film can be easily detected via FL or by the naked eye under a handheld UV lamp at an exposure of 5 ppmv SAS-Cl (Fig. 6). The detection of SAS-Cl in the PS films was fast, occurring in less than one second upon exposure and almost an order of magnitude greater than in solution (5 ppmv vs. 40 ppmv, respectively).

The solution sensitivity of **1** may have been affected by the equilibrium between the imine functionality and the corresponding hydrolyzed amine and pyrene aldehyde products. In the solid

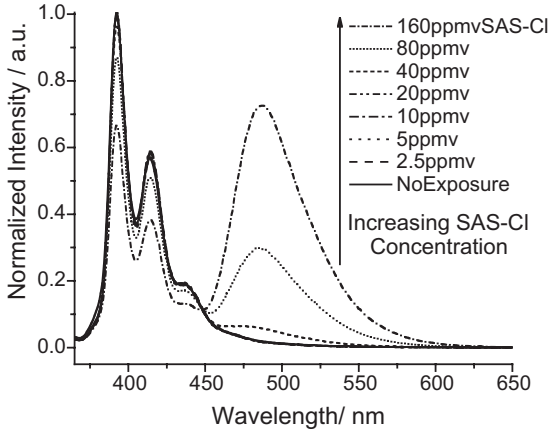

Figure 5. The sensitivity of **1**, at 1×10^{-4} wt % in toluene, to SAS-Cl.

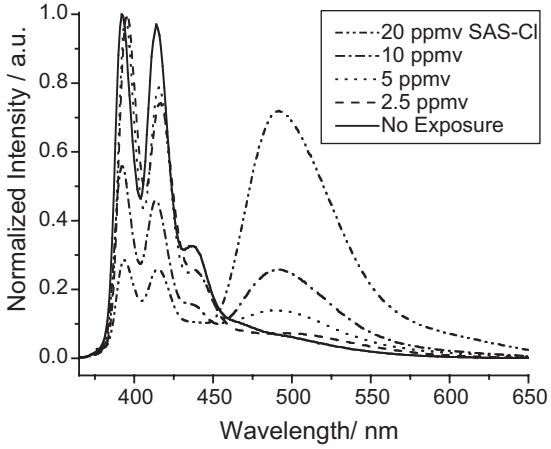

Figure 6. The sensitivity of **1** to SAS-Cl in a PS film, from a solution of 15 wt % PS and 0.1 wt % **1** in toluene.

form **1** is stable, having a shelf life of at least one year, as checked by NMR; however, the equilibrium of **1** with the hydrolyzed amine could be more pronounced in dilute solutions. This hydrolyzed amine would react with SAS-Cl to effectively lower the threshold sensitivity of **1**; amine would react with SAS-Cl, requiring more SAS-Cl to be added to the solution in order to detect the green emission, therefore the sensitivity of **1** in solution would be decreased. Previous work, illustrated by Stern-Volmer constants, showed that diethyl fluorophosphate (fluoro-Sarin surrogate (SAS-F)) was much more reactive than SAS-Cl suggesting that the activity of the organophosphate directly affects the sensitivity of the sensor, thus **1** would be more sensitive to SAS-F versus SAS-Cl.[11] In turn, **1** would be even more sensitive to Sarin itself.

Fluorescence optical microscopy (FOM) of cross-sections of exposed PS films were taken. Interestingly, at lower exposures (less than 20 ppmv SAS-Cl), emission only occurs at the film surface, indicating that the emission of **1** when reacted to SAS-Cl is diffusion dependent (Fig. S5). Sensitivity could be increased if surface area versus the amount of **1** was increased, implying the use of smaller objects such as micrometer and nanofibers would allow for increased sensitivity.[25,28]

The selectivity of **1** in the PS films was determined by exposure to a large excess of various organophosphates and acetyl chloride, with similar structure and functionality to Sarin and its mimic SAS-Cl (Fig. 7). These films containing **1** were determined to be insensitive towards alkyl phosphates (TEP and TBP) or the Soman surrogate (SOS). The selectivity of **1** towards an acid chloride (AcCl) and a dichlorophosphate (PDCP) was also measured. A small response was seen from exposure to AcCl and PDCP, indicating that the increased reactivity of SAS-Cl is significant and why no response was observed upon addition of SOS. The selectivity of **1** in solution was similar to the selectivity in the bulk PS films.

2.3. Fibers: Properties and Applications

Micrometer and sub-micrometer fibers were manufactured using two approaches, direct drawing and electrospinning. As stated earlier, micrometer and nanofibers have great potential for applications in devices for tissue engineering, photonics, catalysis, and sensing. Functional fibers can be electrospun into mesh mats, able to be placed in solutions or airstreams, for applications in sensing systems.[24,25] Suspended, ordered fibers could be incorporated into optical devices for use in electronics, photonics, optics, and sensors[19,20,23] or as scaffolds for microfluidic devices.[20] In addition, fibers have increased surface area and thus have increased exposure to the sensing environment. If sensing in the solid is diffusion limited, smaller objects with increased surface area may prove to be more sensitive.[25,28]

Suspended, ordered micrometer and sub-micrometer fibers were manufactured by a direct and facile approach developed by Cohn and associates.[20,27] As Cohn, McKinley, and coworkers have shown, the drawn fiber diameter can be tailored by the modulation of solution properties including viscosity and surface tension, which are changed by varying the solution concentration and the MW of the polymer.[30,32] In this report, drawn fibers were created from a toluene solution of 15 wt % PS ($M_n = 400$ kDa), containing 0.1 wt % **1**, to form fibers with various diameters from less than 1 μm to approximately 40 μm (Fig. 8). These unexposed fibers (Fig. 8A) were then exposed to SAS-Cl vapor to measure their sensitivity. The green emission of **1** could be easily detected at 2.5 ppmv exposure to SAS-Cl by FOM (Fig. 8B and C) and at 5 ppmv by the naked eye under a handheld UV lamp. The ''turn on'' optical detection event is easily seen in the difference between the unexposed fibers in Figure 8A and the same fibers exposed to SAS-Cl in Figure 8B.

Electrospun fibers were created by spinning a DMF solution of 20 wt % PS ($M_n = 400$ kDa) solution, with 0.13 wt % **1**, flowing at 0.01 mL min^{-1} across a distance of 12 cm with

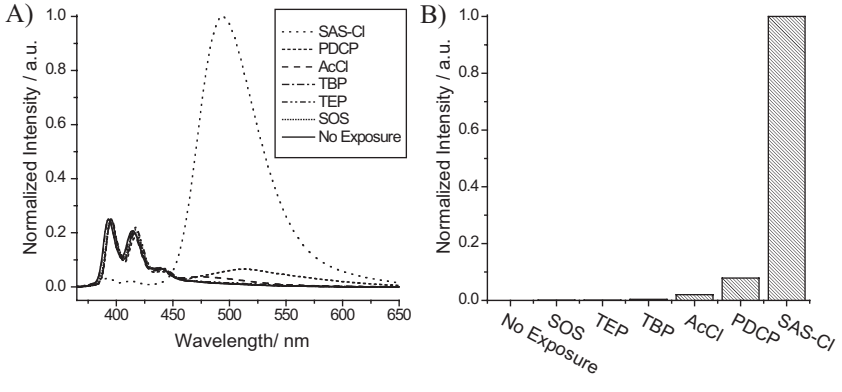

Figure 7. FL spectra (A) and emission intensity at $\lambda = 492$ nm (B) showing the selectivity of **1** in PS films (from a solution of 15 wt % PS and 0.1 wt % **1** in toluene) for SAS-Cl versus other compounds. FL samples were excited at $\lambda_{ex} = 350$ nm. Emission of **1** was measured at $\lambda = 492$ nm nm to determine selectivity in B.

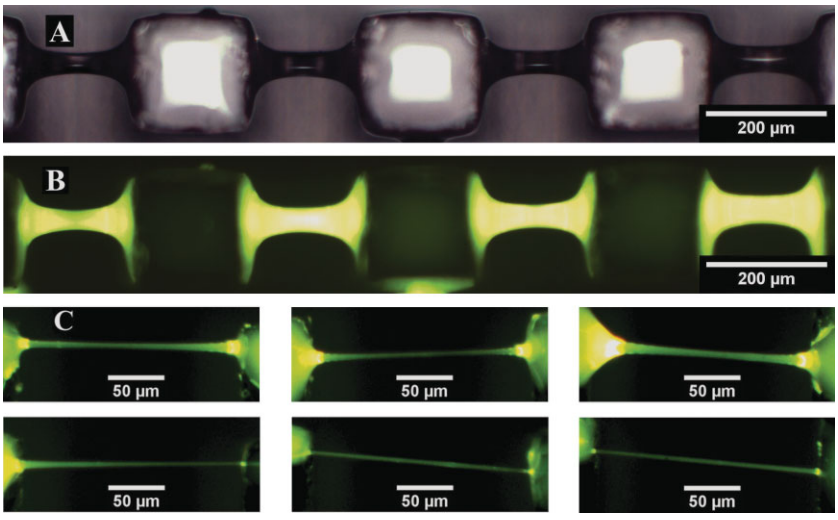

Figure 8. Optical microscopy of PS fibers containing **1** (from a solution of 15 wt % PS and 0.1 wt % **1** in toluene) in bright field illumination with no exposure (A) and in fluorescence after exposure to SAS-Cl (B). FOM of fibers with an average diameter of 4.9 µm after exposure to SAS-Cl (C).

an applied voltage of 16 kV. This concentration of PS and **1** maintains the same composition of PS to **1** in the dried electrospun fibers, as used previously in the PS films and direct drawn, oriented fibers. The resultant fibers formed a mat and have an average diameter of approximately 360 nm with no observed beading (Fig. 9A). As shown in the literature, electrospun polystyrene fiber diameter and morphology can be tuned by molecular weight of the polymer and concentration of the solution (Fig. S6).[26] The sensitivity of the electrospun fibers was examined and the green emission of **1** was detected at 10 ppmv exposure to SAS-Cl as measured by FL (Fig. S7) and 5 ppmv by both FOM (Fig. 9B) and the naked eye under a handheld UV lamp. The high density of fluorescent fibers in the electrospun mat account for the bright green background in the FOM picture of Figure 9B. The slight decrease in sensitivity of the electrospun fibers as compared to the solid and suspended, oriented fibers could have occurred due to slight solvation of the smaller electrospun fibers by the acetone used as a diluent for SAS-Cl.

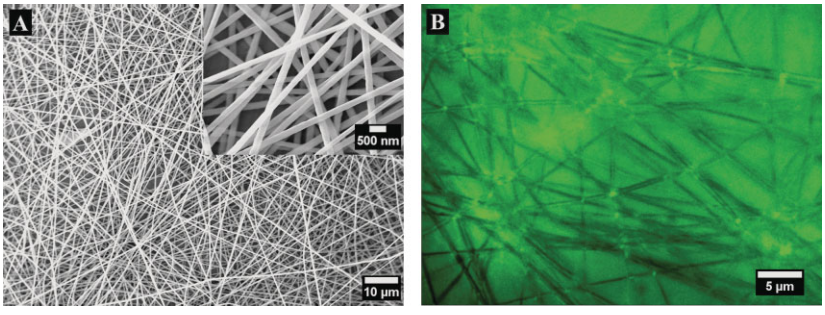

Figure 9. Electrospun PS fibers containing **1** (from a solution of 20 wt % PS and 0.13 wt % **1** in DMF) imaged by SEM (A) and FOM after exposure to SAS-Cl (B).

3. Conclusions

A novel approach for the fluorimetric sensing of nerve agents has been presented. The approach is facile, timely, and easy to interpret via the change from no response to a green emission. The sensitivity of the sensing molecule in solution versus PS films and micrometer and sub-micrometer fibers was found to be 40 and 5 ppmv, respectively. This increase in sensitivity in the solid and fiber states can be attributed to increased local concentration of sensing species in the solid as well as increased surface area and thus exposure to the sensing molecules. The pyrene imine based sensing molecule was found to be selective towards a Sarin surrogate versus other organophosphates, acid chloride, a hydroxyl Soman surrogate (SOS), and less reactive halogenated phosphates. This sensing scheme has the potential to be incorporated into a functional fluorimetric device. The application of this detection into functional micrometer and nanofibers will allow it to be utilized with optical devices and photonics as well as solution and airflow sensing devices.

4. Experimental

Materials: All chemical reagents were purchased from Aldrich, Alfa Aesar, Fisher, Cambridge Isotopes Aldrich, VWR, or Acros Organics and used without further purification unless otherwise stated. Polystyrene (PS) standards of number average molecular weight (M_n) of 400 kDa and polydispersity index (PDI) of 1.06 were purchased from VWR and used for all films and fibers.

[2-(3,5-dioxo-10-oxa-4-aza-tricyclo[5.2.1.0^{2,6}]dec-8-en-4-yl)-ethyl]-carbamic Acid tert-Bbutyl Ester: Di-*tert*-butyl dicarbonate (16.0 g, 73.3 mmol) was added to a solution of ethanol amine (3.96 mL, 66.6 mmol) in dioxane (400 mL) and allowed to stir at room temperature for overnight. The solvent was then removed under reduced pressure and the crude product was redissolved in dichloromethane (200 mL) and washed, consecutively, once with 1% HCl solution (200 mL), twice with a saturated NaCl solution (2 × 100 mL), and once with water (200 mL). The final solution was treated with $MgSO_4$ and the solvent was removed under reduced pressure to afford the (2-hydroxy-ethyl)-carbamic acid *tert*-butyl ester in 98% yields (10.5 g) as colorless oil. (2-Hydroxy-ethyl)-carbamic acid *tert*-butyl ester (4.00 g, 24.8 mmol) was then added to a round-bottom flask charged with 10-oxa-4-aza-tricyclo[5.2.1.0^{2,6}]dec-8-ene-3,5-dione (3.73 g, 22.6 mmol) and triphenylphosphine (6.51 g, 24.8 mmol). Tetrahydrofuran (200 mL) was then added to the flask to dissolve the mixture. The flask was immersed in an ice bath upon which diisopropyl azodicarboxylate (4.8 mL, 24.8 mmol) was added dropwise. The ice bath was then removed and the reaction mixture was allowed to stir at room temperature for 12 h. The solvent was later removed under reduced pressure. The pure product, [2-(3,5-dioxo-10-oxa-4-aza-tricyclo[5.2.1.0^{2,6}]dec-8-en-4-yl)-ethyl]-carbamic acid *tert*-butyl ester, was isolated by crystallization from anhydrous diethyl ether (5.58 g, 80% yield). ^{1}H NMR (300 MHz) and ^{13}C NMR (75 MHz) spectra were obtained using a Bruker DPX-300MHz NMR spectrometer. ^{1}H NMR (300 MHz, $CDCl_3$, δ): 6.48 (s, 2H), 5.22 (s, 2H), 4.80

(br s, 1H), 3.61–3.57 (m, 2H), 3.29–3.23 (m, 2H), 2.82 (s, 2H), 1.37 (s, 9H); ^{13}C NMR (75 MHz, $CDCl_3$, δ): 176.26, 155.87, 136.41, 80.93, 79.65, 47.33, 38.71, 38.42, 28.27.

1: [2-(3,5-Dioxo-10-oxa-4-aza-tricyclo[5.2.1.0^{2,6}]dec-8-en-4-yl)-ethyl]-carbamic acid *tert*-butyl ester (2.00 g, 18.0 mmol) was dissolved in a 2.5 M HCl solution of dioxane (10.0 mL). The solution was allowed to stir at room temperature for 6 h. The product was filtered and washed three times with 20 mL diethyl ether and dried under vacuum to afford 2-(3,5-dioxo-10-oxa-4-aza-tricyclo[5.2.1.0^{2,6}]dec-8-en-4-yl)-ethyl-ammonium chloride as a white powder (1.40 g, 80% yield). To a round-bottom flask charged with 2-(3,5-dioxo-10-oxa-4-aza-tricyclo[5.2.1.0^{2,6}]dec-8-en-4-yl)-ethyl-ammonium chloride (1.40 g, 14.4 mmol), 1-pyrenecarboxaldehyde (3.98 g, 17.3 mmol), absolute ethanol (50 mL), and triethylamine (4.0 mL, 28.8 mmol) were added. The reaction mixture was refluxed for 30 min and the product crystallized upon cooling the solution to room temperature. The product, 4-{2-[(pyren-1-ylmethylene)-amino]-ethyl}-10-oxa-4-aza-tricyclo[5.2.1.0^{2,6}]dec-8-ene-3,5-dione (**1**), was isolated by filtration as yellow crystals (5.45 g, 90% yield). ^{1}H NMR (300 MHz, $CDCl_3$, δ): 9.16 (s, 1H), 8.89 (d, $J = 9.3$ Hz, 1H), 8.44 (d, $J = 7.9$ Hz, 1H), 8.21–7.98 (m, 7H), 6.38 (s, 2H), 5.16 (s, 2H), 4.01 (s, 4H), 2.79 (s, 2H); ^{13}C NMR (75 MHz, $CDCl_3$, δ): 176.26, 162.10, 136.38, 131.14, 130.56, 129.83, 128.61, 128.32, 127.39, 126.75, 126.05, 125.79, 125.58, 124.86, 124.71, 124.54, 122.82, 80.75, 59.14, 47.35, 39.62.

2: To a round-bottom flask charged with 1-pyrenecarboxaldehyde (2.00 g, 8.69 mmol), absolute ethanol (50 mL) and 1-ethylpropylamine (1.51 g, 17.4 mmol) were added. The reaction mixture was refluxed for 30 min and the solvent was removed under reduced pressure. The unreacted 1-ethylpropylamine was removed at 100 °C under vacuum. The viscous brown oil was dissolved in dichloromethane, passed through a short silica plug, and dried under vacuum to afford (1-ethyl-propyl)-pyren-1-ylmethylene amine (**2**) as a yellow solid (2.21 g, 85% yield). ^{1}H NMR (300 MHz, $CDCl_3$),δ): 9.25 (s, 1 H), 8.86 (d, $J = 9.3$ Hz, 1H), 8.39 (d, $J = 7.9$ Hz, 1H), 8.22–7.99 (m, 7 H), 3.12 (m, 1H), 1.84–1.75 (m, 4H), 0.96 (t, $J = 7.2$ Hz, 6H); ^{13}C NMR (75 MHz, $CDCl_3$, δ): 158.08, 132.54, 131.26, 130.26, 129.69, 129.20, 128.53, 128.33, 127.51, 126.41, 126.09, 125.77, 125.53, 124.98, 124.75, 122.80, 76.10, 29.03, 11.22.

Sensitivity and Selectivity Measurements: All UV-Vis spectra were obtained with a PerkinElmer Lambda 2 series spectrophotometer with PECSS software, below an absorbance value of 1.0 to obey the Beer-Lambert law. Fluorescence (FL) measurements were performed on a Jobin Yvon Fluorolog-3 fluorimeter, using samples of absorbance values less than 0.1 to avoid aggregation phenomena. Samples were excited at $\lambda_{ex} = 350$ nm and emission was measured from $\lambda_{em} = 365$–650 nm at a right angle to the excitation.

Sensitivity measurements of the **1** in solution were taken at 1×10^{-4} wt % in dimethylsulfoxide (DMSO), chloroform ($CHCl_3$), and toluene. Specific amounts of SAS-Cl diluted with the corresponding solvent were added and the response was measured via FL. All sensitivities were measured in parts per million volume (ppmv) using corresponding volumetric amounts of SAS-Cl versus the volume of the container used. For film sensitivity of **1**, 0.1 wt % of **1** was added to toluene. This solution was then added to PS to form a 15 wt % solution. The PS/**1** solution (20 μL) was dropped onto a quartz slide and toluene was allowed to evaporate to form a film. The slide was placed in a closed cuvette, with known volume, and positioned in the fluorimeter to have excitation and emission at 45 degrees to the surface. Specific amounts of SAS-Cl, diluted in acetone as a carrier agent, were added to the cuvette and the response was measured via FL. The selectivity of **1** in solution and film was measured in the same manner except a large excess (20 μL), as compared to molecules of **1**, of each reagent was added to the cuvette. All sensitivity and selectivity measurements were normalized to the intensity at $\lambda = 392$ nm of their corresponding spectra with no exposure of any reagent.

Fiber Drawing: Direct drawing was performed by Drawing 20 μL of 15 wt % PS and 0.1 wt % **1** dissolved in toluene, applied to a glass cover slip, over a glass array of 200 × 200 μm square pillars with 200 μm spacing. Electrospinning of PS was performed using 10 mL syringe equipped with an 18 gauge (inner diameter = 0.838 mm) blunt-tipped needle. An aluminum foil collector (~ 10 × 10 cm) was placed at a separation distance of 12 cm. Fibers were spun using a flow rate of 0.01 mL/min with applied voltages of 12, 16, and 20 kV. Fibers were drawn using two solutions, 15 wt % PS and 0.1 wt % **1** as well as 20 wt % PS and 0.13 wt % **1** dissolved in *N*,*N*-dimethylformamide (DMF). Surface morphology, diameter, and fiber morphology (beading) were checked via scanning electron microscopy (SEM).

Microscopy: All optical microscopy images were taken using an Olympus BXS1 upright microscope equipped with a HBO-100 Hg lamp. Fluorescence optical microscopy (FOM) images were taken using a $\lambda_{ex} = 420$–480 nm excitation filter and a $\lambda_{em} = 520$–800 nm emission filter. SEM was performed on a JEOL 6320 FXV Field Emission SEM with JEOL Orion software.

Acknowledgements

The authors thank the Presidential Early Career Awards for Scientists and Engineers (PECASE), the Army Research Office for the Young Investigator Award, and the National Science Foundation's Nanoscale Interdisciplinary Research Team (NSF NIRT, Grant 0506941) for their generous support of this work. The authors thank Scott D. Cambron from the University of Louisville for fabricating the glass pillar arrays and Dr. SungCheal Moon from the University of Massachusetts, Amherst for help with electrospinning. Supporting Information is available online from Wiley InterScience or from the author.

Received: July 8, 2008
Revised: November 10, 2008
Published online: January 29, 2009

[1] a) E. Croddy, *Jane's Intelligence Rev.* **1995**, *7*, 520. b) H. Nozaki, N. Aikawa, *Lancet* **1995**, *345*, 1446. c) T. Suzuki, H. Morita, K. Ono, K. Maekawa, R. Nagai, Y. Yazaki, *Lancet* **1995**, *345*, 980.
[2] R. M. Black, R. J. Clarke, R. W. Read, M. T. J. Reid, *J. Chromatogr. A* **1994**, *662*, 301.
[3] M. Thompson, ''Rotting Rockets'', *Time* **1996**, *147*.
[4] a) H. O. Michel, E. C. Gordon, J. Epstein, *Environ. Sci. Technol.* **1973**, *7*, 1045. b) T. J. Novak, L. W. Daasch, J. Epstein, *Anal. Chem.* **1979**, *51*, 1271.
[5] V. Pavlov, Y. Xiao, I. Willner, *Nano Lett.* **2005**, *5*, 649.
[6] K. J. Wallace, J. Morey, V. M. Lynch, E. V. Anslyn, *New J. Chem.* **2005**, *29*, 1469.
[7] a) T. J. Dale, J. Rebek, *J. Am. Chem. Soc.* **2006**, *128*, 4500. b) S. W. Zhang, T. M. Swager, *J. Am. Chem. Soc.* **2003**, *125*, 3420. c) D. Knapton, M. Burnworth, S. J. Rowan, C. Weder, *Angew. Chem. Int. Ed.* **2006**, *45*, 5825.
[8] E. R. Menzel, L. W. Menzel, J. R. Schwierking, *Talanta* **2005**, *67*, 383.
[9] R. J. Russell, M. V. Pishko, A. L. Simonian, J. R. Wild, *Anal. Chem.* **1999**, *71*, 4909.
[10] M. Burnworth, S. J. Rowan, C. Weder, *Chem. Eur. J.* **2007**, *13*, 7828.
[11] R. Shunmugam, G. N. Tew, *Chem. Eur. J.* **2008**, *14*, 5409.
[12] K. J. Wallace, R. I. Fagbemi, F. J. Folmer-Andersen, J. Morey, V. M. Lynth, E. V. Anslyn, *Chem. Commun.* **2006**, 3886.
[13] M. B. Pushkarsky, M. E. Webber, T. Macdonald, C. K. N. Patel, *Appl. Phys. Lett.* **2006**, *88*, 044103.
[14] W. E. Steiner, S. J. Klopsch, W. A. English, B. H. Clowers, H. H. Hill, *Anal. Chem.* **2005**, *77*, 4792.
[15] a) A. J. Russell, J. A. Berberich, G. E. Drevon, R. R. Koepsel, *Annu. Rev. Biomed. Eng.* **2003**, *5*, 1. b) J. A. Ashley, C. H. Lin, P. Wirsching, K. D. Janda, *Angew. Chem. Int. Ed.* **1999**, *38*, 1793.
[16] a) A. L. Jenkins, O. M. Uy, G. M. Murray, *Anal. Commun.* **1997**, *34*, 221. b) A. L. Jenkins, O. M. Uy, G. M. Murray, *Anal. Chem.* **1999**, *71*, 373. c) A. L. Jenkins, R. Yin, J. L. Jensen, *Analyst* **2001**, *126*, 798.
[17] a) N. A. Rakow, A. Sen, M. C. Janzen, J. B. Ponder, K. S. Suslick, *Angew. Chem. Int. Ed.* **2005**, *44*, 4528. b) N. A. Rakow, K. S. Suslick, *Nature* **2000**, *406*, 710.
[18] R. C. Smith, A. G. Tennyson, M. H. Lim, S. J. Lippard, *Org. Lett.* **2005**, *7*, 3573.

[19] a) H. Q. Liu, J. B. Edel, L. M. Bellan, H. G. Craighead, *Small* **2006**, *2*, 495. b) L. M. Tong, R. R. Gattass, J. B. Ashcom, S. L. He, J. Y. Lou, M. Y. Shen, I. Maxwell, E. Mazur, *Nature* **2003**, *426*, 816. c) M. R. Stan, P. D. Franzon, S. C. Goldstein, J. C. Lach, M. M. Ziegler, *Proc. IEEE* **2003**, *91*, 1940.

[20] S. A. Harfenist, S. D. Cambron, E. W. Nelson, S. M. Berry, A. W. Isham, M. M. Crain, K. M. Walsh, R. S. Keynton, R. W. Cohn, *Nano Lett.* **2004**, *4*, 1931.

[21] C. Drew, X. Y. Wang, K. Senecal, H. Schreuder-Gibson, J. N. He, J. Kumar, L. A. Samuelson, *J. Macromol. Sci. Pure Appl. Chem.* **2002**, *39*, 1085.

[22] R. Dersch, M. Steinhart, U. Boudriot, A. Greiner, J. H. Wendorff, *Polym. Adv. Technol.* **2005**, *16*, 276.

[23] a) D. P. O'Neal, M. A. Meledeo, J. R. Davis, B. L. Ibey, V. A. Gant, M. V. Pishko, G. L. Cote, *IEEE Sens. J.* **2004**, *4*, 728. b) Y. Wang, W. H. Liu, K. M. Wang, G. L. Shen, R. Q. Yu, *Fresenius J. Anal. Chem.* **1998**, *360*, 702.

[24] a) C. Drew, X. Liu, D. Ziegler, X. Y. Wang, F. F. Bruno, J. Whitten, L. A. Samuelson, J. Kumar, *Nano Lett.* **2003**, *3*, 143. b) X. Y. Wang, C. Drew, S. H. Lee, K. J. Senecal, J. Kumar, L. A. Samuelson, *J. Macromol. Sci. Pure Appl. Chem.* **2002**, *39*, 1251. c) X. Y. Wang, Y. G. Kim, C. Drew, B. C. Ku, J. Kumar, L. A. Samuelson, *Nano Lett.* **2004**, *4*, 331.

[25] X. Y. Wang, C. Drew, S. H. Lee, K. J. Senecal, J. Kumar, L. A. Sarnuelson, *Nano Lett.* **2002**, *2*, 1273.

[26] a) G. Eda, S. Shivkumar, *J. Appl. Polym. Sci.* **2007**, *106*, 475. b) T. Jarusuwannapoom, W. Hongroijanawiwat, S. Jitjaicham, L. Wannatong, M. Nithitanakul, C. Pattamaprom, P. Koombhongse, R. Rangkupan, P. Supaphol, *Eur. Polym. J.* **2005**, *41*, 409.

[27] S. Pabba, A. N. Siclorov, S. M. Berry, M. M. Yazdanpanah, R. S. Keynton, G. U. Sumanasekera, R. W. Cohn, *ACS Nano* **2007**, *1*, 57.

[28] a) P. Gibson, H. Schreuder-Gibson, D. Rivin, *Colloids Surf. A* **2001**, *187*, 469. b) D. H. Reneker, I. Chun, *Nanotechnology* **1996**, *7*, 216.

[29] R. Shunmugam, G. J. Gabriel, C. E. Smith, K. A. Aamer, G. N. Tew, *Chem. Eur. J.* **2008**, *14*, 3904.

[30] S. M. Berry, S. A. Harfenist, R. W. Cohn, R. S. Keynton, *J. Micromech. Microeng.* **2006**, *16*, 1825.

[31] a) I. Abdellah, E. Ibrahim, R. Farag, *Gazz. Chim. Ital.* **1988**, *118*, 141. b) A. N. El-Khazandar, *Phosphorus Sulfur Silicon Relat. Elem.* **1997**, *126*, 243.

[32] A. Tripathi, P. Whittingstall, G. H. McKinley, *Rheol. Acta* **2000**, *39*, 321.

ADVANCED FUNCTIONAL MATERIALS

DOI: 10.1002/adfm.200800947

Fluorimetric Nerve Gas Sensing Based on Pyrene Imines Incorporated into Films and Sub-micron Fibers

By *Jeremy M. Rathfon*, *Zoha M. AL-Badri*, *Raja Shunmugam*, *Scott M. Berry*, *Santosh Pabba*, *Robert S. Keynton*, *Robert W. Cohn*, and *Gregory N. Tew**

[*] Prof. Gregory N. Tew, Jeremy M. Rathfon, Dr. Zoha M. AL-Badri, Raja Shunmugam
Department of Polymer Science and Engineering
University of Massachusetts Amherst
120 Governors Drive
Amherst, Massachusetts 01003
E-mail: tew@mail.pse.umass.edu
Scott M. Berry, Santosh Pabba, Prof. Robert S. Keynton, Prof. Robert W. Cohn
ElectroOptics Research Institute and Nanotechnology Center
University of Louisville
Louisville, Kentucky 40292

Supporting Information

I. Characterization

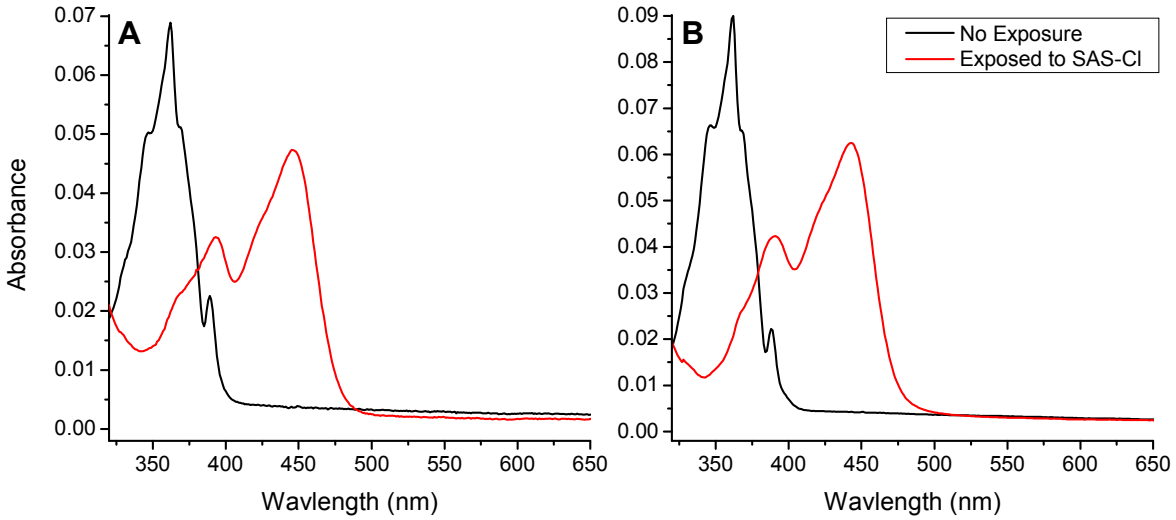

Figure S1. UV-Vis spectra of **1** (A) and **2** (B) in toluene before and after exposure to a large excess (20 µL) of SAS-Cl.

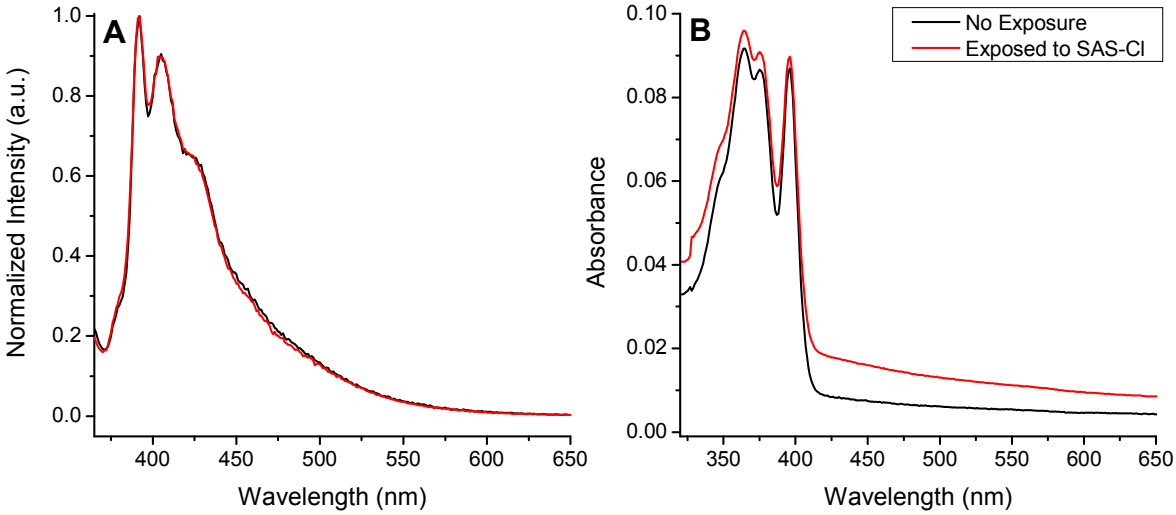

Figure S2. FL (A) and UV-Vis (B) spectra of 1-pyrenecarboxaldehyde in toluene before and after exposure to a large excess (20 µL) of SAS-Cl.

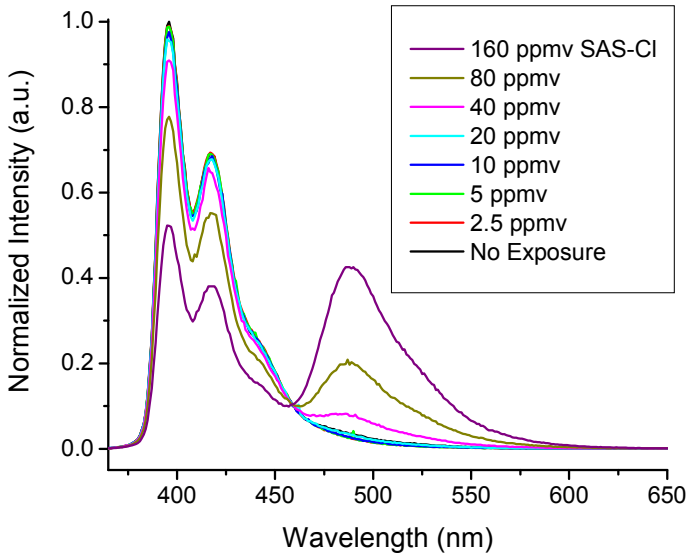

Figure S3. The sensitivity of **1**, at 1 x 10^{-4} wt % in $CHCl_3$, to SAS-Cl.

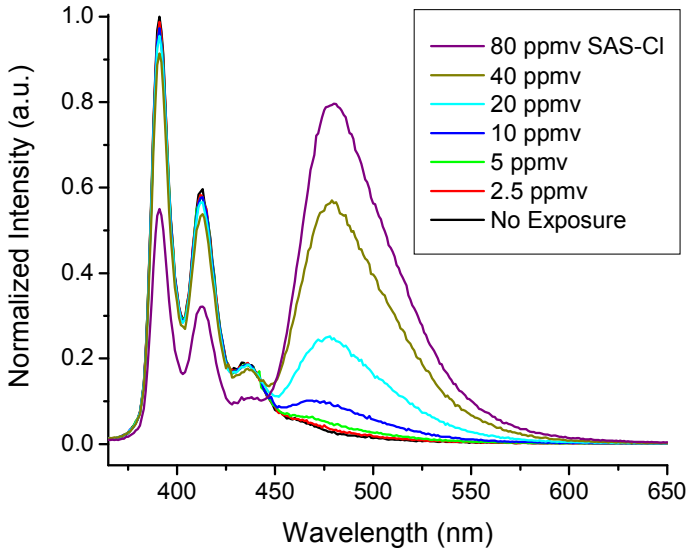

Figure S4. The sensitivity of **2**, at 1 x 10^{-4} wt % in toluene, to SAS-Cl.

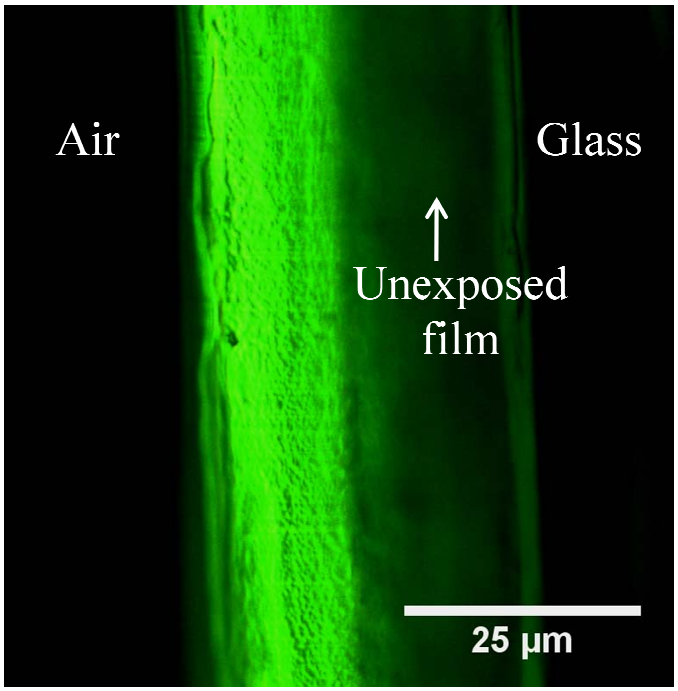

Figure S5. FOM of a PS film cross-section ~ 34 µm thick with partial exposure to SAS-Cl (~ 5 ppmv SAS-Cl). Film formed from a solution of 15 wt % PS and 0.1 wt % **1** in toluene.

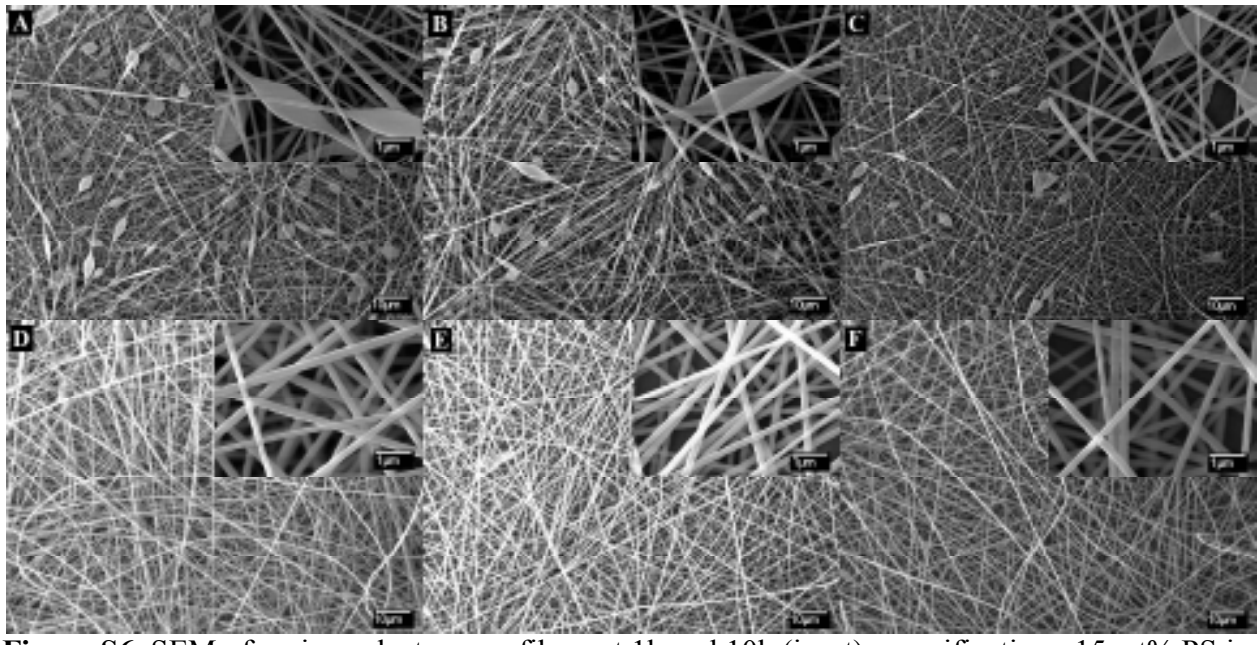

Figure S6. SEM of various electrospun fibers at 1k and 10k (inset) magnification. 15 wt% PS in DMF containing 0.1 wt% **1** at 12 (A), 16 (B), and 20 (C) kV applied voltage. 20 wt% PS in DMF containing 0.13 wt% **1** at 12 (D), 16 (E), and 20 (F) kV applied voltage.

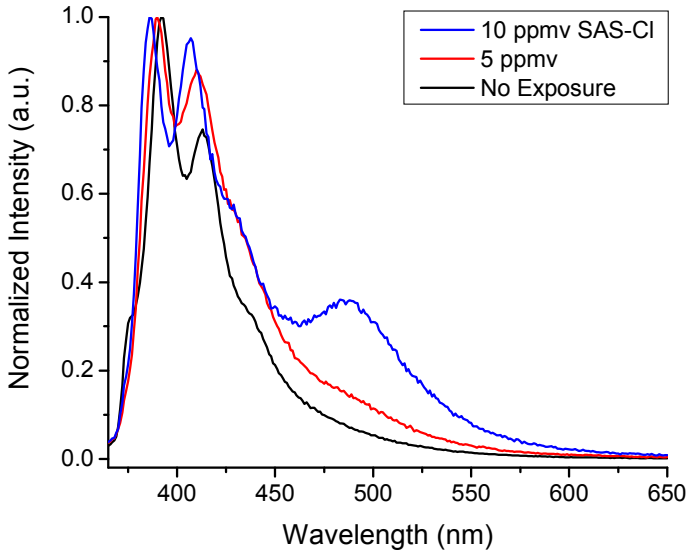

Figure S7. The sensitivity of **1** to SAS-Cl in electrospun PS fibers, from a solution of 20 wt % PS and 0.13 wt % **1** in DMF.

II. ^{1}H and ^{13}C NMR

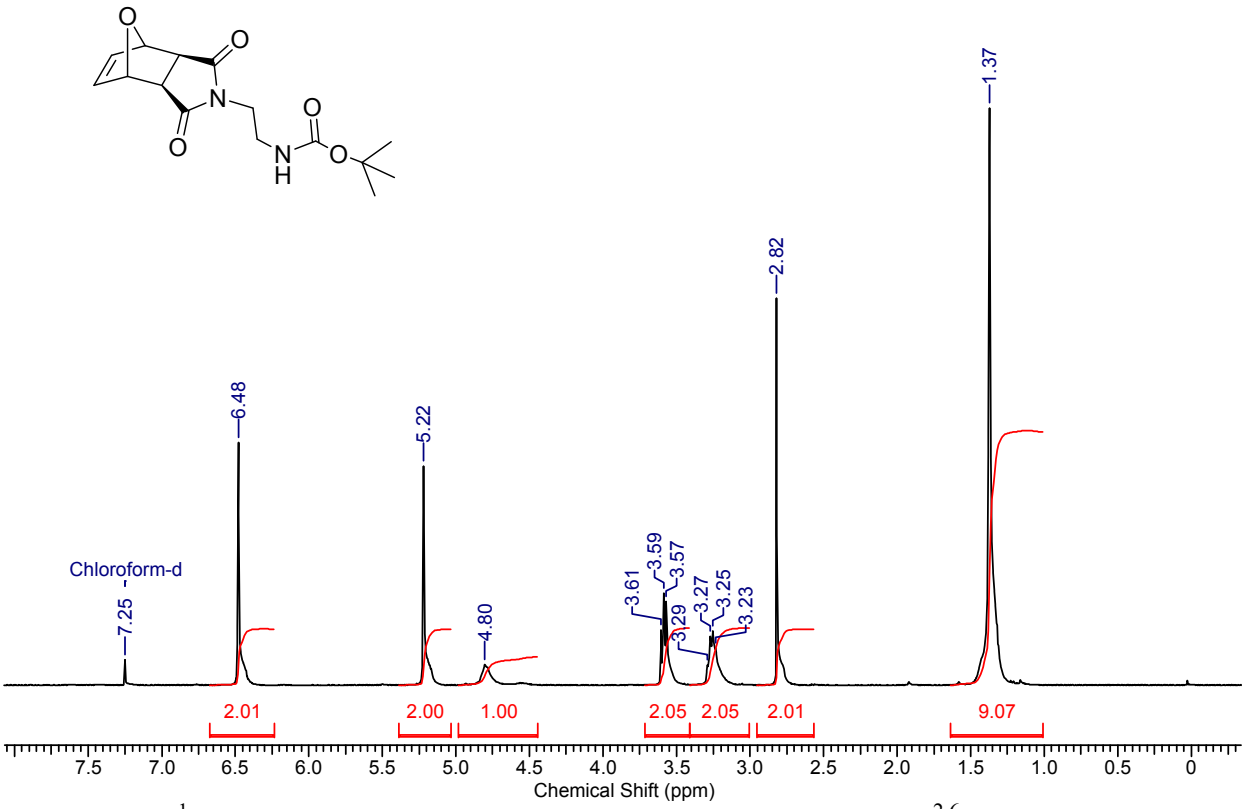

Figure S8. ^{1}H NMR of [2-(3,5-dioxo-10-oxa-4-aza-tricyclo[5.2.1.0^{2,6}]dec-8-en-4-yl)-ethyl]-carbamic acid *tert*-butyl ester in $CDCl_3$.

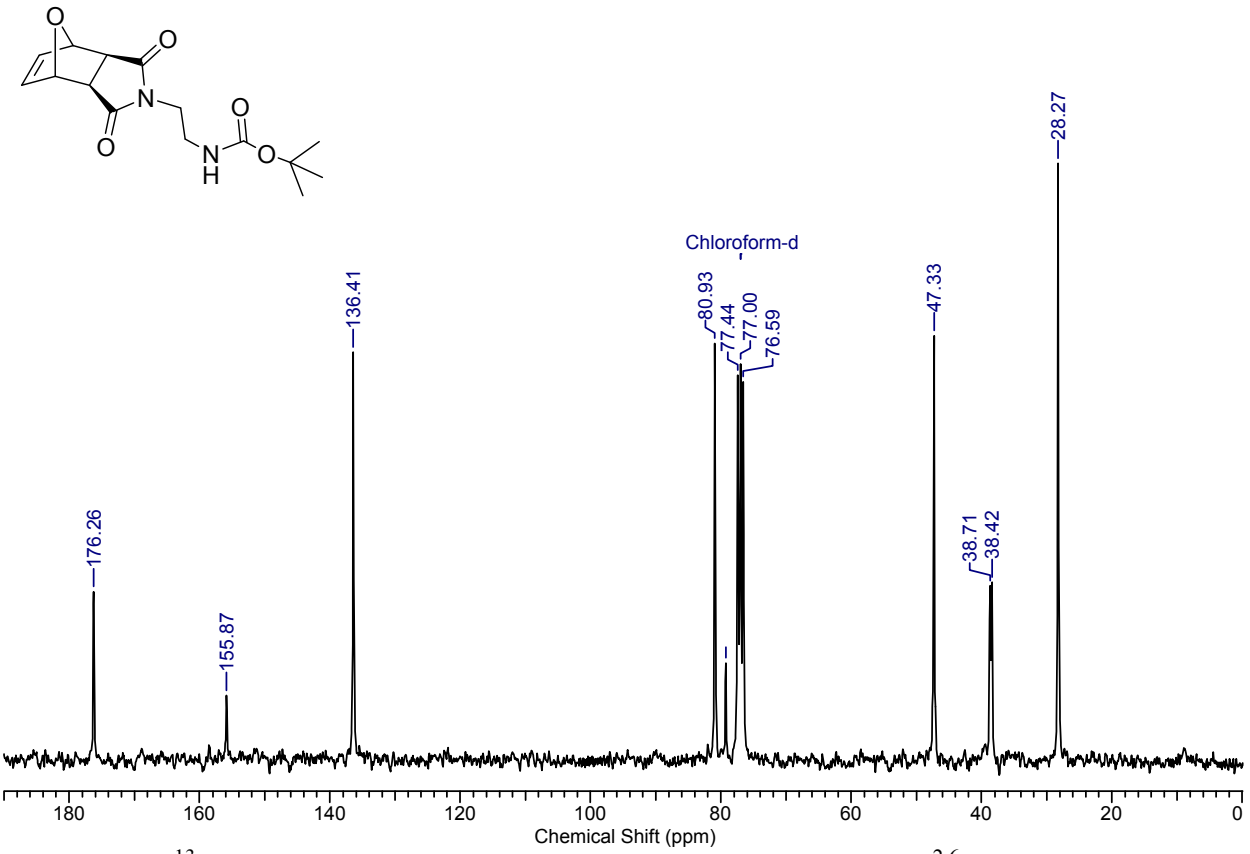

Figure S9. ^{13}C NMR of [2-(3,5-dioxo-10-oxa-4-aza-tricyclo[5.2.1.$0^{2,6}$]dec-8-en-4-yl)-ethyl]-carbamic acid *tert*-butyl ester in $CDCl_3$.

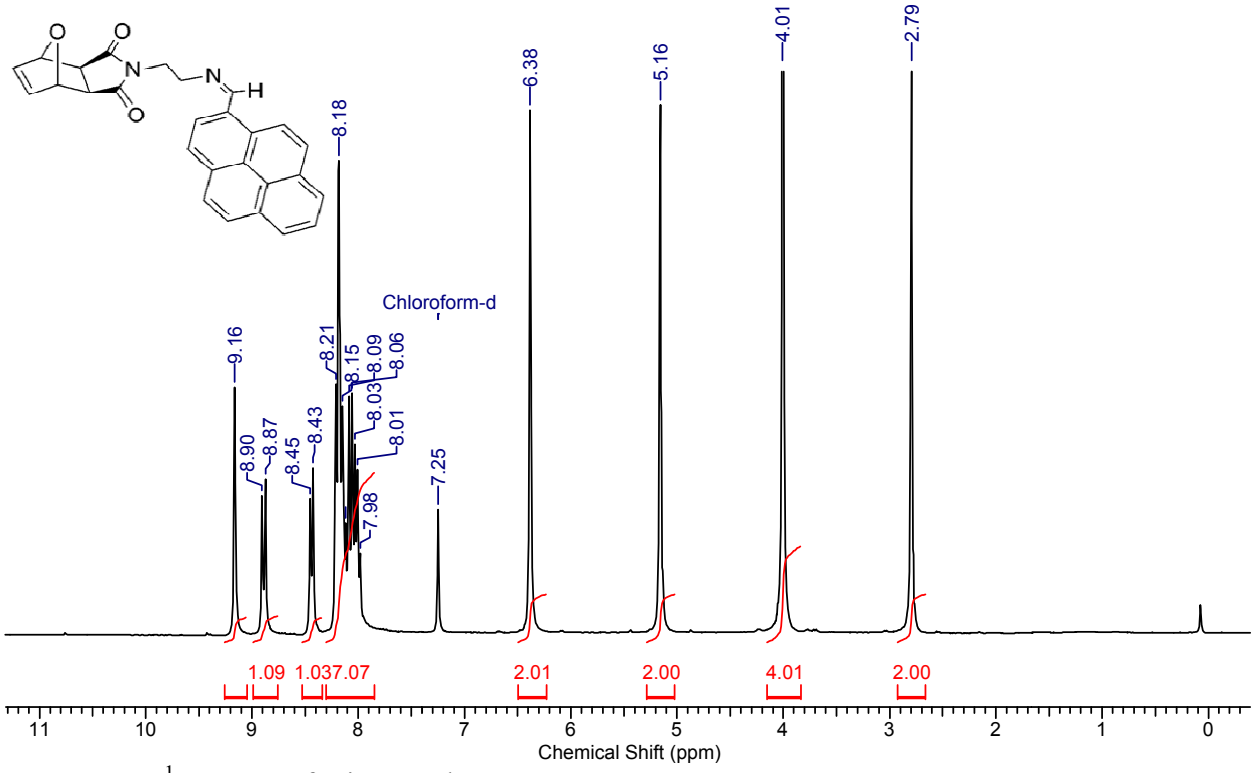

Figure S10. ^{1}H NMR of **1** in $CDCl_3$.

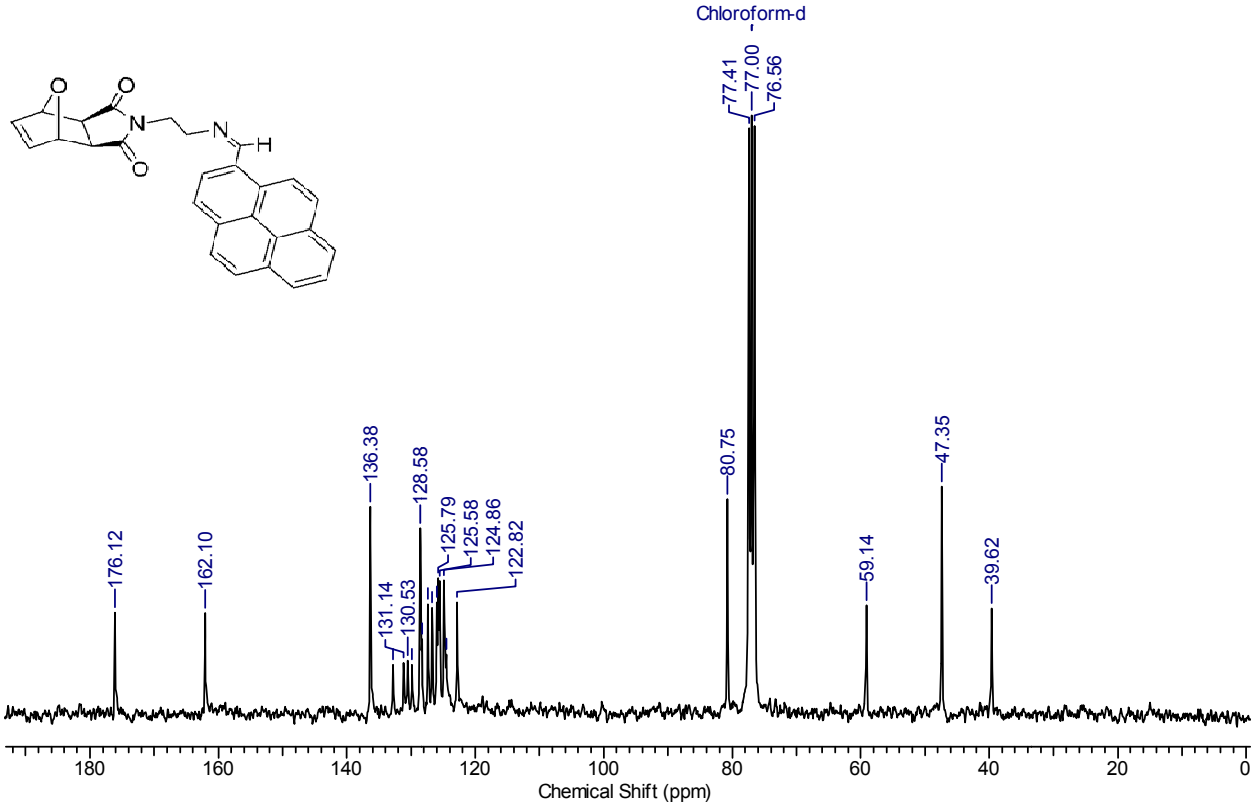

Figure S11. ^{13}C NMR of **1** in $CDCl_3$.

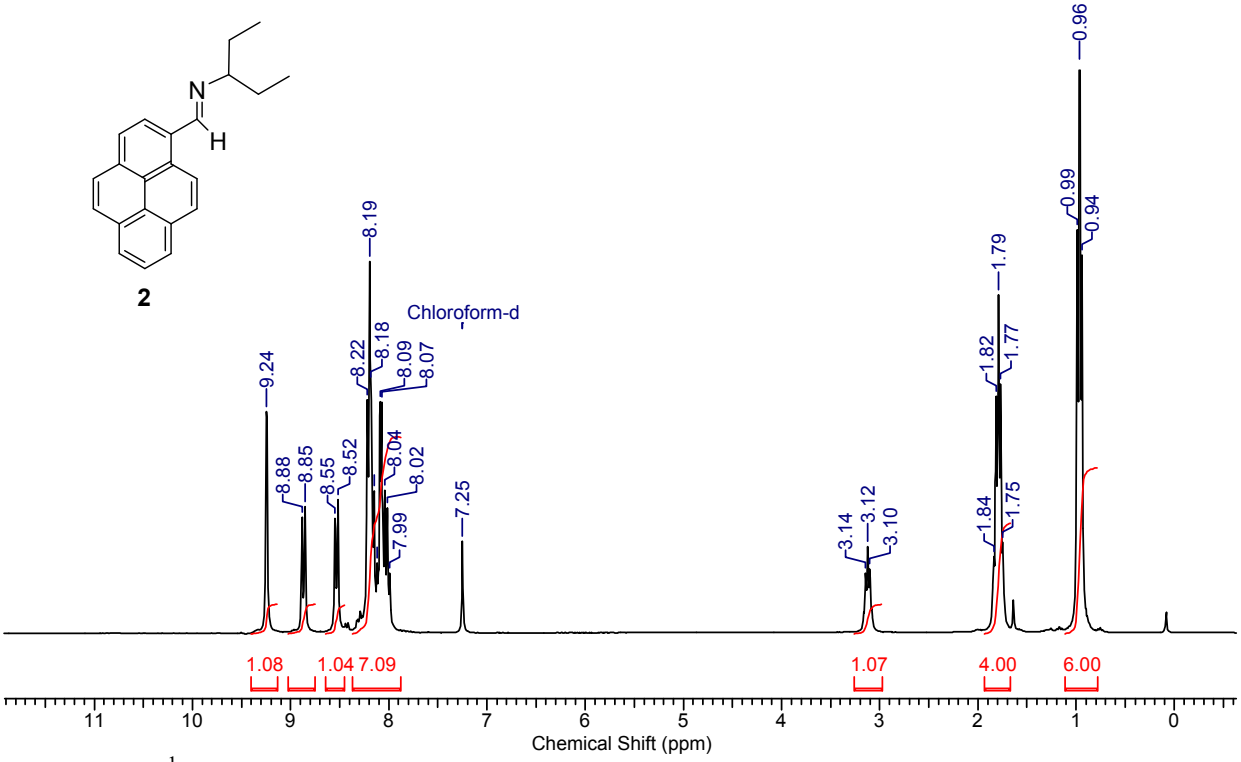

Figure S12. ^{1}H NMR of **2** in $CDCl_3$.

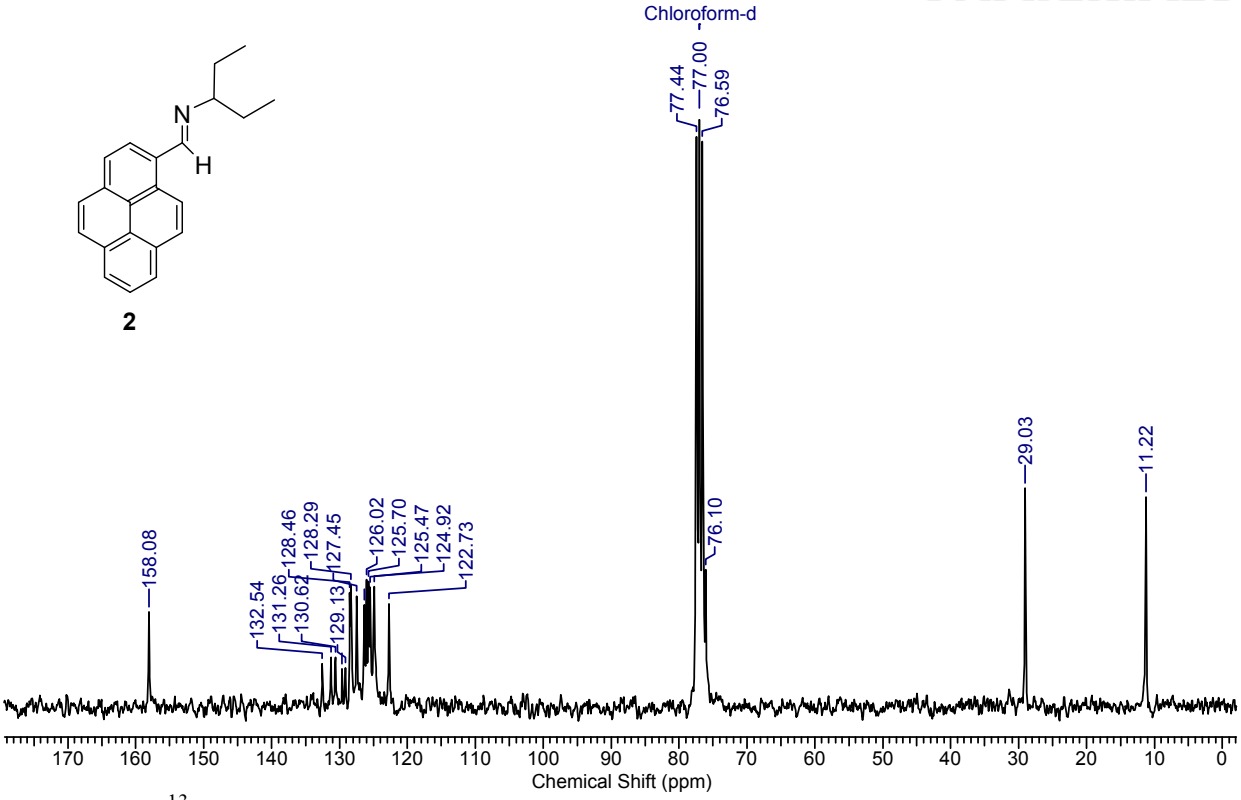

Figure S13. ^{13}C NMR of **2** in $CDCl_3$.

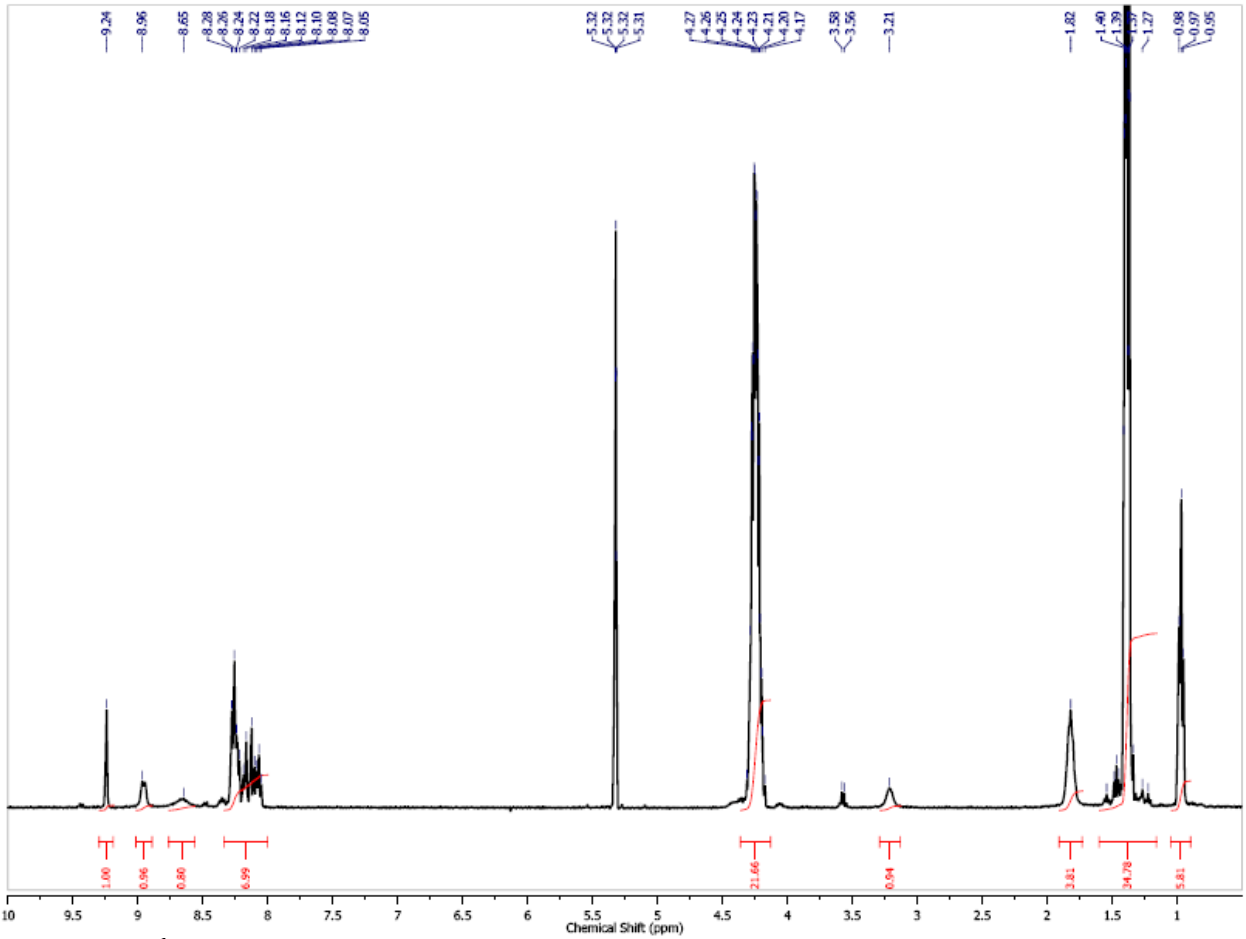

Figure S14. ^{1}H NMR of **2** exposed to SAS-Cl in CD_2Cl_2.